# **Integrated In-Ear Device for Auditory Health Assessment**

Akshay Paul<sup>1</sup>, Abraham Akinin<sup>1</sup>, Min S. Lee<sup>1</sup>, Matthew Kleffner<sup>2</sup>, Stephen R. Deiss<sup>1</sup>, and Gert Cauwenberghs<sup>1</sup>

Abstract—Clinical assessment of the human auditory system is an integral part of evaluating the health of a patient's cognitive processes. Conventional tests performed by audiologists include the Auditory Steady State Response (ASSR) and the Auditory Brainstem Response (ABR), both of which present an audio stimulus to the patient in order to elicit a change in brain state measurable by electroencephalography (EEG) techniques. Spatial monitoring of the electrophysiological activity in the auditory cortex, temporal cortex, and brain stem during auditory stimulus evaluation can be used to pinpoint to location of auditory dysfunction along the auditory pathway. However, given the obtrusive nature of conventional auditory evaluation techniques and the lack of information about sound transduction and cochlear dynamics usually irrecoverable by EEG, a better approach is needed to improve its clinical utility. Here, we present an in-ear device for auditory health assessment that integrates a sound engine for stimulation and high-density dry-electrode EEG for real-time simultaneous recording of brain activity. This system provides ease-of-use and patient comfort. We also investigate the auditory transfer function of the hearing system as an intricate convolution of the tympanic membrane, middle ear bones, and the cochlear subsystems.

#### I. Introduction

# A. Auditory System

The human auditory system utilizes mechanical and electrical processes to sense, filter, and amplify sound pressure waves to electrical impulses in the brain. Dysfunction and disease can impact the performance of any or all portions of the auditory pathway, producing serious and often, confounding pathology. In the cases of patients presenting symptoms of tinitus, for example, dysfunction can occur at the cochlear hair cells, in the auditory nerves, the brainstem, or even in the auditory cortex. Localization and isolation of the cause and location of the disease state is difficult with conventional ASSR and ABR techniques because information is lost [1].

The frequency domain representation of the time dependent acoustic wave at the ear,  $a_{in}(t)$ , is

$$A_{in}(j\omega) = \mathcal{F}\{a_{in}(t)\}\tag{1}$$

where  $\mathcal{F}$  denotes the Fourier Transform. The acoustic pressure wave at the entrance of the cochlea is then:

$$A_{co}(j\omega) = H_{tym}(j\omega) H_{oss}(j\omega) A_{in}(j\omega)$$
 (2)

where  $H_{tym}$  and  $H_{oss}$  represent the transfer functions describing the transduction of the auditory signals in the tympanic membrane and ossicles of the middle ear. The inner

hair cells in the cochlea then *channelize* this into thousands of different channels of progressive frequency. Their outputs along the auditory nerve thus convey a high-dimensional ( $N \approx 30,000$ ) sample of the spectrum

$$[A_{co}(j\omega_0), A_{co}(j\omega_1), \dots A_{co}(j\omega_N)]$$
 (3)

for subsequently complex processing in the auditory cortex. Thus if we are interested in measuring physiological benchmarks of audition (as opposed to behavioral and cognitive feedback tests), we must interrogate the auditory cortex response. However, despite recent advances, we are only able to distinguish macroscopic signals generated by the brain when we perform non-invasive, wearable electroencephalography (EEG). The signals recorded at each surface electrode have undergone many non-linear transformations from that cochlear 'bus' through the cortical layers of processing, and the local fields evoked by their neural activations are significantly spread through volume conduction. The EEG signal  $E_i$  at any particular surface electrode i:

$$E_i(j\omega) = \sum_{n=1}^{N} c_{in} \ A_{co}(j\omega_n)$$
 (4)

where  $c_{in}$  are linear coefficients of the spectral maps on the EEG recording surface (normally the scalp, and here specifically, the ear canal) compounding the cochlear/auditory transfer function and the observable resulting brain response. Since this mixture does not retain any distinguishable frequency information we must modulate the input signal  $A_{co}$ 's spectrum narrowly and apply the techniques of frequency domain system identification [2].

### B. ASSR and EEG

The auditory steady state response (ASSR) is a valuable test because it provides audiologists an assessment of a subject's hearing as a function of frequency. The nature of the stimulus, a repeating set of tones or broadband noise stimulus that is modulated in amplitude by a lower frequency, elicits robust auditory cortex activity which can then be measured in a non-invasive manner from externally placed electrodes. Further, because the steady state auditory stimulus is often presented for extended period of time, on the order of several minutes, the resulting oscillation recorded from the brain are generally subject-state independent. The capability to directly measure the physiology, as opposed to subjective behavioral feedback by an engaged patient, is another major reason for the use of ASSR in auditory assessment of infant and non-responsive subjects [1].

<sup>&</sup>lt;sup>1</sup>Department of Bioengineering, Jacobs School of Engineering, and Institute for Neural Computation, UC San Diego, La Jolla, CA 92093, USA.

<sup>2</sup>Signal Processing Research Department, Starkey, Eden Prairie, MN 55344, USA. Dayton, OH 45435, USA

### C. In-Ear EEG

Recent efforts have been made to improve auditory evaluation that utilize precisely engineered stimulation sound profiles to efficiently evaluate hearing across a wide range of frequencies. In-ear EEG has been demonstrated to be an effective alternative to scalp EEG for certain sensing applications, including auditory stimulus response [3]–[5]. Furthermore, dry-contact electrodes in the ear canal [6] have proven effective in picking up skin conductivity in addition to auditory EEG signals [7], permitting extended biomedical use [8], [9] in continuous health monitoring. The main advantages of in-ear dry-electrode EEG over conventional scalp EEG are improved user comfort, reduced body area contact, discretion [10]- [13], and closer proximity to auditory processes [3]–[6].

## D. Aim of study

In this study, we aimed to demonstrate the feasibility of a fully integrated in-ear device, capable of presenting auditory stimuli, recording brain activity, and providing enhanced details about the state of a subject's auditory health.

Further, we provide a mathematical model for sound transduction in the human auditory system, laying the foundation for improved localization of auditory dysfunction from EEG measurements.

#### II. METHODS

### A. Data and Subjects

Data was gathered for the studies presented here as part of an ongoing study assessing the performance of in-ear electrophysiology as a wearable health sensing platform and an alternative for conventional geometry EEG. Auditory evoked potentials were measured in 32 trials from each ear of 2 healthy subjects, following experimental procedures in Institutional Review Board approved protocols.

# B. Integrated Ear Molds

- 1) Shells: Custom-fitted earpieces were fabricated for the subjects' ears using advanced 3D printing techniques and microelectronics assembly (Figure 1). Ear impressions used to produce the precisely fitting earpieces were taken by an licensed audiologist and transformed into a 3D digital point clouding using a laser scanner. A standard two-part molding compound used for the custom fitting of hearing aids was injected past the secondary bend of each subject's ear canals and out on to the meatus and concha. The point cloud data was imported into 3D CAD software to create the smooth surface entities of the earpiece and were precisely fitted with hole features for the electrodes to maintain high-density and uniform spacing.
- 2) Electrodes: Earpieces were fitted with 17 custom fabricated dry-contact Ag/AgCl electrodes, each with a diameter of 2 mm. A flexible 30 AWG insulated wire was soldered to each electrode and embedded into the lumen of the earpiece. Of the 17 electrodes, 8 serve as in-canal sensors, 8 as concha cavum and cymba sensors, and 1 as a non-sensing drivenright-leg (DRL). Electrodes protrude slightly past the surface



Fig. 1. The earpieces fabricated from 3D CAD models of the subject's ear shown here embedded with 17 Ag-Ag/Cl electrodes each. A air tube comes through the lumen of the earpieces the provide sound directly the ear canal.

of the earpiece and are spaced far enough apart to prevent inadvertent shorting. A small cantilever fitted internally to each electrode provides an adequate spring force to ensure proper electrode-skin contact during wear.

3) Audio: Auditory stimuli were generated in MATLAB using standard audiology practices. Specifically, steady-state sound stimuli were generated using broadband uniform white noise amplitude modulated 100 percent by low frequencies ranging from 10 to 100 Hz (Figure 2). A Blackman window algorithm was utilized to create the amplitude modulation pattern. Sound stimulus was presented to subjects at 75 dB through an air tube for 6 minutes. An air tube sound transducer was used to ensure precise control over stimuli intensity and frequency, and not prevent microphonic interference.

### C. Acquisition Systems

Real-time measurements of skin conductance activity at multiple sites on the body were managed simultaneously by a low-noise, multichannel biosignal amplifier and analog-to-digital converter (ADC) (Texas Instruments ADS1299) [14]. Four ADC chips were utilized on a custom designed printed circuit board (PCB) capable of 32-channel recording with on-board filtering, bias drive, and current sources. With 16 custom wet or dry configurable electrodes for the ear and 4 conventional adhesive gel electrodes placed on the palm and fingers, skin conductance was mapped in these areas.

Mapping of skin conductance in the ear canal was achieved by programmatically selecting pairs of electrodes and passing a fixed alternating current across using the ADCs programmable gain amplifier (PGA). A pull-up and pull-down current source was connected to the positive and negative electrodes, respectively, and the resulting voltage measured by the channel amplifier was recorded. The next permutation of the two-electrode configuration was selected and the process was repeated.

# D. Setup of ASSR

Auditory steady state responses from the auditory cortex of test subjects were measured binaurally from the in-ear devices for 8 stimulus frequencies (20, 30, 40, 50, 70, 80, 90, and 100 Hz). Audio was present at 75 dB for exactly

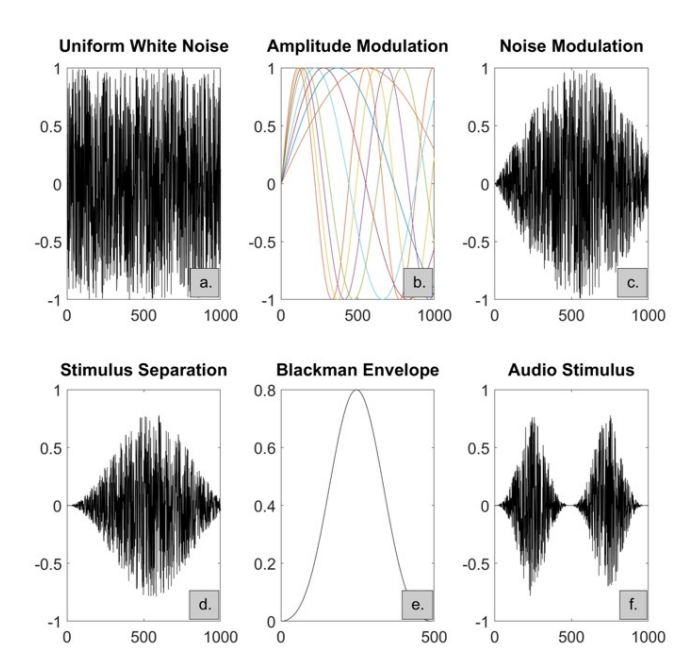


Fig. 2. Auditory sound stimuli were designed for the ASSR study in a series of steps following the conventional audiology process for audio engineering stimuli. Uniformly distributed white noise (a.) is first generated in software and then convolved with a set of sinusoids (b.), each at one of the frequencies listed in Part D. of the Methods section, producing an amplitude modulated white noise signal (c.). Superimposed waveforms are separated from the modulated noise signal into frequency-specific amplitude modulations (d.). A Blackman enveloped, as shown in (e.) is applied to the separated waveforms, producing an appropriately shaped and timed final sound stimulus (f.). In (f.) is depicted the complete 40 Hz ASSR audio used in this study.

6 minutes per frequency tested. EEG measurements were recorded at a sampling frequency of 1,000 Hz across all 32 channels and streamed wirelessly to the Linux computer. Using EEGLAB, saved data was bandpass filtered from 2 to 100 Hz to remove unwanted high frequency signals and reduce noise. The power spectral density (PSD) of the EEG data was calculated to evaluate the subject's hearing response to the steady state sound stimulus. Peaks in the PSD were generally observed at 60 Hz, representing line noise in North America, at 10 Hz, the EEG alpha band, and the stimulus AM frequency.

### III. RESULTS

The auditory steady state trials performed at the test frequencies produced characteristic power spectra, as measured by the in-ear EEG. The baseline EEG recording taken with a still subject receiving no auditory stimulus results in a PSD with a strong 60 Hz peak, as expected, but with no other discernible peaks above 20 Hz. The EEG data is band-pass filtered between 2 and 120 Hz, so no spectral information was observed beyond 120 Hz. High amplitudes are observed for frequencies lower than 20Hz, which is normal and expected for EEG because of the strong alpha band (8 Hz–12 Hz) generated in the brain during eye closure, and as a consequence of 1/f noise.

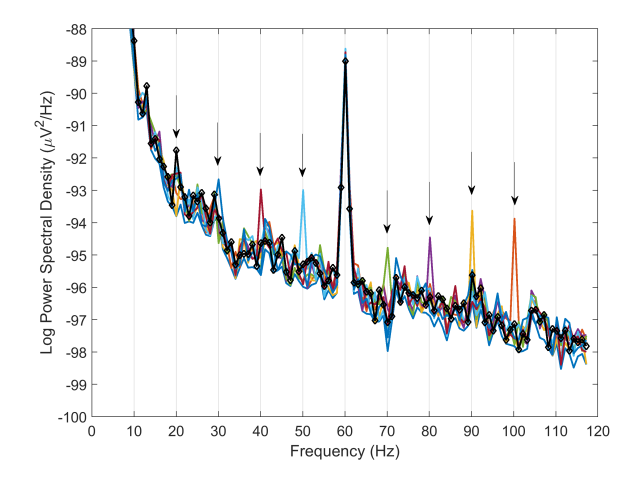


Fig. 3. The result of the ASSR test frequencies with the top being baseline—no sound presented. Below that is 100 Hz, 90 Hz, 80 Hz, 70 Hz, 50 Hz, 40 Hz, 30 Hz, and 20 Hz responses to amplitude modulated steady state auditory stimuli.

When the subject was presented with a 100 Hz amplitude modulated broadband noise stimulus for a sustained 6 minutes, a clear peak in the EEG PSD at 100 Hz is observed (Figure 3). The same characteristics peak is seen at 90 Hz in the PSD of EEG recordings from the 90 Hz amplitude modulated auditory stimulus. Note that both 100 Hz and 90 Hz peak are clearly of greater power than the PSD noise level, with the very strong 60 Hz line noise peak shown as a reference. Peaks at 80 Hz and 70 Hz in the EEG PSD, each corresponding to its respective auditory stimulus frequency, display a noticeably diminished peak power, despite the sound level (75 dB) of the auditory stimulus being presented to the subject remaining constant across all stimuli.

An auditory stimulus with amplitude modulation of 60 Hz was forgone for obvious reasons of interference from line noise. Peaks at 50 Hz and 40 Hz in the PSD also clearly showed a measured response from the subjects' auditory cortex. These peaks are clearly defined above the PSD noise level, but are still less in power than the higher frequency amplitude modulation frequencies. Diminished further in power are 30 Hz and 20 Hz peaks, with the 20 Hz auditory response barely above the PSD noise level. Finally, a 10 Hz amplitude modulation was tested but is not discernible in the results because of high power seen in this low frequency region from the subjects' eyes being closed (alpha waves).

In parallel to in-ear EEG, conventional scalp EEG recordings were made using a commercial 30-electrode headset. PSDs calculated from EEG recordings made during the 40 Hz and 90 Hz auditory stimuli (Figure 4) depict a clear peak, above the noise floor at their respective stimulus frequencies. These scalp EEG results are consistent with the expectations from a conventional ASSR study.

# IV. CONCLUSION

The EEG PSD shows stability over an extended recording session with different auditory frequencies being presented

and the occasional change in subject state. The in-ear EEG is able to consistently measure the steady-state brain activity arising from the subjects' temporal lobes in response to the presented auditory stimuli. This system is able elicit and detect steady-state responses with confidence in the test frequency range of 20 to 100 Hz, producing a PSD with comparable performance and frequency features as a commercial scalp EEG device. The negligible changes observed in overall PSD noise level and consistent amplitude of the 60 Hz peak, used here as a reference, suggests the absence of microphonic interference from the integrate sound transducer and resilience of the system to changes in electrode-skin conditions overtime.

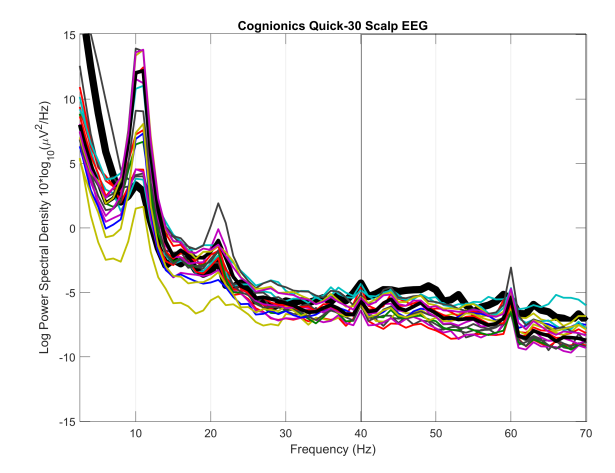
Deconvolving the auditory stimulus amplitude modulation frequency from the resulting EEG PSD peak by diving in the frequency domain would provide useful information regarding the auditory transfer function, as discussed earlier. The perceived linear relationship in ASSR between sound and oscillations in the auditory cortex could be further expanded to account for the dynamics of the tympanic membrane, the middle ossicles, the cochlear transduction, and the middle brain stem latency. In fact, the ASSR tests performed in this study could even elucidate the involvement of the brain stem in the auditory pathway as seen by the higher power in EEG PSD from amplitude modulation frequencies greater than 70 Hz, a most likely evidence of a middle brain stem latency.

### ACKNOWLEDGMENT

The authors thank members of the Integrated Systems Neuroengineering laboratory in the Department of Bioengineering at UC San Diego, including Jun Wang for assistance in PCB assembly.

### REFERENCES

- [1] W. Lobitz Jr and C. Campbell, "Physiology of the glands of the human ear canal: Preliminary report," *Journal of Investigative Dermatology*, 19(2), 125-135, 1952.
- [2] A. Akinin, N. Govil, H. Poizner, and G. Cauwenberghs, "Frequency domain identification of proprioceptive evoked potentials in compliant kinematic experiments," 2015 7th International IEEE/EMBS Conference on Neural Engineering (NER), Montpelier, France, 2015.
- [3] D. Looney et al., "An in-the-ear platform for recording electroencephalogram," 2011 Ann. Int. Conf. IEEE Engineering in Medicine and Biology Society (EMBc'2011), Boston, MA, 2011.
- [4] D. Looney et al., "The In-the-Ear Recording Concept: User-Centered and Wearable Brain Monitoring," in *IEEE Pulse*, vol. 3, no. 6, pp. 32-42, Nov. 2012.
- [5] V. Goverdovsky, W. Rosenberg, T. Nakamura, D. Looney, D. Sharp, C. Papavassiliou, M. Morrell, and D. Mandic, "Hearables: Multimodal physiological in-ear sensing," in *Scientific Reports*, 7:6948, July 2017.
- [6] Xiong Zhou, Qiang Li, S. Kilsgaard, F. Moradi, S. L. Kappel and P. Kidmose, "A wearable ear-EEG recording system based on drycontact active electrodes," 2016 IEEE Symposium on VLSI Circuits (VLSI'2016), Honolulu, HI, 2016.
- [7] Paul, A., Deiss, S., Tourtelotte, D., Kleffner, M., Zhang, T., and Cauwenberghs, G., "Electrode-Skin Impedance Characterization of In-Ear Electrophysiology Accounting for Cerumen and Electrodermal Response," *IEEE EMBS Int. Conf. Neural Engineering (NER19)*, 2019.
- [8] Gruzelier, J. H., and Venables, P. H., "Skin conductance orienting activity in a heterogeneous sample of schizophrenics," *Journal of Nervous and Mental Disease*, 155(4), 277-287, 1972.



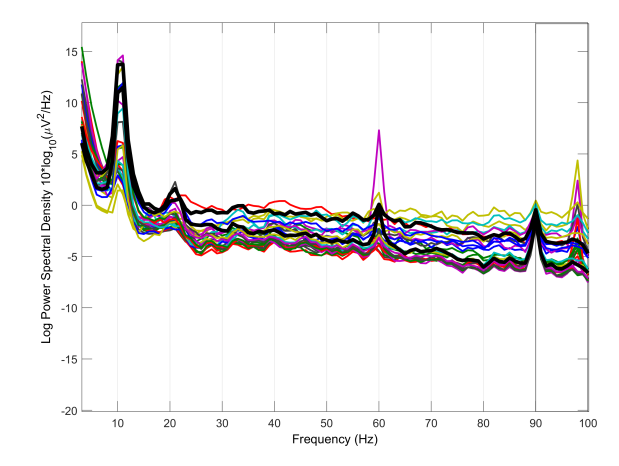


Fig. 4. Power spectral density (PSD) of scalp EEG recordings made during the ASSR in-ear study using a commercial, Cognionics Quick-30 dry-contact electrophysiology system. Two PSDs are shown here for comparison to the in-ear EEG PSD shown in Fig. 3, with the first (Top) showing EEG results from the 40 Hz auditory stimulus and the second (Bottom) showing results from the 90 Hz stimulus. A weighted black line is added to the Quick-30 channels with to greatest correlation to the in-ear EEG based on electrode location and direction.

- [9] C. Tronstad, O. Elvebakk, H. Kalvy, M. R. Bjrgaas and Ö. G. Martinsen, "Detection of sympathoadrenal discharge by parameterisation of skin conductance and ECG measurement," 2017 39th Annual International Conference of the IEEE Engineering in Medicine and Biology Society (EMBC), Seogwipo, pp. 3997-4000, 2017.
- [10] T. J. Sullivan, S. R. Deiss and G. Cauwenberghs, "A Low-Noise, Non-Contact EEG/ECG Sensor," 2007 IEEE Biomedical Circuits and Systems Conference, Montreal, Quebec, pp. 154-157, 2007.
- [11] Y.M. Chi, T.P. Jung and G. Cauwenberghs, "Dry-Contact and Non-contact Biopotential Electrodes: Methodological Review," in *IEEE Reviews in Biomedical Engineering*, vol. 3, pp. 106-119, 2010.
- [12] Y. M. Chi and G. Cauwenberghs, "Wireless Non-contact EEG/ECG Electrodes for Body Sensor Networks," 2010 International Conference on Body Sensor Networks, Singapore, pp. 297-301, 2010.
- [13] Y. M. Chi, Y. T. Wang, Y. Wang, C. Maier, T. P. Jung and G. Cauwenberghs, "Dry and Noncontact EEG Sensors for Mobile Brain-Computer Interfaces," in *IEEE Transactions on Neural Systems and Rehabilitation Engineering*, vol. 20, no. 2, pp. 228-235, March 2012.
- [14] Texas Instruments ADS1299. Technical Datasheet (2016).